Received: 7 October 2022 | Revised: 7 December 2022 | Accepted: 3 January 2023

DOI: 10.1111/sum.12881

Soil Use and Management | WILEY

RESEARCH PAPER

Simulating the soil phosphorus dynamics of four long-term field experiments with a novel phosphorus model

S. Anton A. Gasser[1] | **Kerstin Nielsen**[2] | **Bettina Eichler-Löbermann**[3] | **Martin Armbruster**[4] | **Ines Merbach**[1] | **Uwe Franko**[1]

[1]Helmholtz Centre for Environmental Research GmbH – UFZ, Halle (Saale), Germany

[2]Lebenswissenschaftliche Fakultät, Institut für Agrar-und Stadtökologische Projekte an der Humboldt-Universität zu Berlin (IASP), Berlin, Germany

[3]Agronomy and Crop Science, University of Rostock, Rostock, Germany

[4]Agricultural Analytical and Research Institute Speyer (LUFA Speyer), Speyer, Germany

Correspondence
S. Anton A. Gasser, Helmholtz Centre for Environmental Research GmbH – UFZ, Theodor-Lieser-Straße 4, 06120 Halle (Saale), Germany.
Email: anton.gasser@ufz.de

Funding information
Fachagentur Nachwachsende Rohstoffe

Abstract

Phosphorus is a nonrenewable resource, which is required for crop growth and to maintain high yields. The soil P cycle is very complex, and new model approaches can lead to a better understanding of those processes and further guide to research gaps. The objective of this study was to present a P-submodel, which has been integrated in the existing Carbon Candy Balance (CCB) model that already comprises a C and N module. The P-module is linked to the C mineralization and the associated C-pools via the C/P ratio of fresh organic material. Besides the organic P cycling, the module implies a plant-available P-pool (P_{av}), which is in a dynamic equilibrium with the nonavailable P-pool (P_{na}) that comprises the strongly sorbed and occluded P fraction. The model performance was tested and evaluated on four long-term field experiments with mineral P fertilization, farmyard manure as organic fertilizer and control plots without fertilization. The C dynamics and the P_{av} dynamics were modelled with overall good results. The relative RMSE for the C was below 10% for all treatments, while the relative RMSE for P_{av} was below 15% for most treatments. To accommodate for the rather small variety of available P-models, the presented CNP-model is designed for agricultural field sites with a relatively low data input, namely air temperature, precipitation, soil properties, yields and management practices. The CNP-model offers a low entry threshold model approach to predict the C-N and now the P dynamics of agricultural soils.

KEYWORDS

CNP-model, soil P dynamics, soil process modelling, total P and available P

1 | INTRODUCTION

In the last decades, a lot of effort has been made to analyse carbon and nitrogen cycling in soil and to develop models, which represent those processes. A further key element for plant nutrition is P, which is responsible for plant growth, reproduction and energy transfer within the plant. In agriculture, mineral P is used as fertilizer but P reservoirs are limited and depleting (Sulieman & Mühling, 2021; Yan et al., 2022). Therefore, P cycling gains a rising interest in agricultural praxis. Hereby, the application of organic amendments can be an essential part in closing the P cycle. Besides fertilization, P occurs naturally in bedrock and is slowly released through weathering of P-bearing

minerals (Dzombak & Sheldon, 2020). For some regions, P input through deposition can play an important input factor (Vet et al., 2014); however, erosion and leaching processes are an important output pathway where P can get lost into hydrological systems (Alewell et al., 2020).

In soils, P occurs in different species. Water dissolved P, which is directly plant available, while weakly adsorbed P can be made available by plants, for example, through root exudates. Furthermore, P can be bound to aluminium (AL) or iron (FE) complexes or organic compounds. The organic bound P is linked to the C cycle and occurs in biomolecules, such as nucleic acids, phosphoproteins, sugar phosphates and inositol phosphates (Wang et al., 2021). There is a wide variety of analytical extraction method for different P species like calcium acetate-extractable P, double lactate-extractable P, Olsen P and Mehlich 3, just to mention some (Wuenscher et al., 2016).

While those measurable P species represent the extraction method, in model approaches P species often get aggregated in conceptional pools which interact with each other. The choice of pools has to be adapted to the complexity of the analysed system, the data input and the evaluation between complexity and sufficient accuracy. There are some models addressing P turnover in soils: the DDPS model (dynamic phosphorus pool simulator) comprises two pools on spatial scale with annual steps (Sattari et al., 2012; Zhang et al., 2017), whereas the APLE (Annual P Loss Estimator) model calculates the P dynamics on annual scale with three inorganic P-pools and an organic one (Vadas et al., 2012). The LePA (legacy phosphorus assessment) model considers three inorganic P-pools with P fluxes on annual steps (Yu et al., 2021). However, none of these models considers the organic P cycle separately. In DDPS, organic P is assumed to be part of the labile and stable P-pools but it is not considered that P gets released during mineralization of C or bound during the building up of soil organic matter (SOM). APLE assumes a fix rate of organic P, which is not mineralized at the end of the year, not considering, environmental conditions, the date of application nor chemical composition of the organic amendments. Neither do they calculate the crop P uptake, rather fix numbers are assigned (DDPS; Sattari et al., 2012) or the soil P content is used to calculate crop uptake with linear regressions, which are site specific (LePA; Yu et al., 2021).

The P-model approach presented in this paper is integrated into the existing CCB model (Franko et al., 2011), which already comprises C and N modules and targets arable soils requiring small data input on a monthly time scale. From now on, this model is labelled as CNP-model. In addition to the mineral P fractions, the new P-module also deals with an organic P fraction, where the P turnover is coupled to the C mineralization of the three SOM pools of the CNP-model. Notably, each fresh organic matter (FOM) input is characterized by specific mineralization parameters and a FOM-specific C/P ratio. Furthermore, the P-module describes an easily available P (P_{av}) fraction, which is considered as plant-available pool. The P_{av}-pool acts as active pool, which is responsible for the translocation of P into other pools and serves as first sink for P inputs. The P_{av}-pool is in a dynamic equilibrium with the nonavailable pool (P_{na}), which represents the bound and occluded P species. All P associated with the SOM pools, the P_{av}-pool and the P_{na}-pool, form together the total P fraction.

Long-term field experiments (LTE) are most suitable for examining P fertilization management on the soil P status. They enable studying complex fertilizer turnover processes in soils operating on long time scales under environmental conditions. Thus, they provide an overview of the effectiveness of fertilizer management on nutrient mobilization, transformation, translocation and uptake by crops (Siebers et al., 2021). Furthermore, LTEs provide sufficient data to validate model concepts for P dynamics, which are not as easily predictable as C and N dynamics because of high complexity.

For this study, four LTEs were used to evaluate the P-model. The LTEs are located across Germany with different soil types and have different crop rotations. The input data requirement for the CNP-model is relatively low needing air temperature, precipitation, crop yields and management (e.g. ploughing, irrigation, time of seeding and harvest), fertilizer inputs, as well as soil properties like clay and silt content, bulk density and initial values for C and P. The model validation was performed on control plots without fertilizer amendments, mineral fertilized plots and plots with farmyard manure (FYM) as organic fertilizer. Thus, common mineral and organic treatments are used to evaluate the model performance. Moreover, the model is tested on nonfertilized plots to conclude about anthropogenic unsupplied P soil processes.

Agricultural process models can serve as tool to conclude about nutrient dynamics and can help to identify research gaps and provide practical support for farmers and stakeholders. Therefore, the aim of this study was to present the P soil model approach, to validate its performance and to test the model concept on different soils, and management practices.

The main objectives of this study were as follows:

I Introduce and describe the P-model concept.
II Validate the P-module on four long-term field experiments with control plots, mineral fertilization and organic fertilization, with different soil properties.
III Evaluate the model performance compared with the field measurements.

2 | MATERIALS AND METHODS

2.1 | Field trials

Four different field trials were considered for the model evaluation. The field trials were situated across Germany, in Bad Lauchstädt (BL) in Saxony-Anhalt, Berge (BG) in Berlin, Speyer (SP) in Rhineland-Palatinate and Rostock (RO) Mecklenburg Western Pomerania. The required weather data were received from the closest weather station to the test site.

The validation of the P-model was conducted on the control plots (CRL), plots with mineral fertilization (MIN) and plots with farmyard manure (FYM) application. A brief overview is given in Table 1.

In the LTEs of BG, BL and RO, the available P species was measured as double lactate soluble P (DL-P), since this is common for the northern part of Germany. Because of the replacement of the DL-P method, the values were transformed to calcium acetate lactate soluble P (CAL-P) following van Laak et al. (2018) using the equation:

$$\mathrm{CAL_P}\left(\mathrm{mg}*\mathrm{kg}^{-1}\right) = 8 + 0.61 * \mathrm{DL_P}\left(\mathrm{mg}*\mathrm{kg}^{-1}\right) \quad (1)$$

2.1.1 | Berge (BG)

The field trial was set up in March 2011 with a one-factorial randomized block design, with four replications. The crop rotation was as follows: winter rye as whole crop silage followed by maize and in the next year winter rye as whole crop and silage–sorghum. Fertilizers were applied twice a year before the sowing of either rye or maize/sorghum. Furthermore, it is to be noticed that all treatments have been cultivated with winter wheat and mustard as intercrop with an N-fertilization of 100 kg N ha^{-1} as premanagement.

The fertilizer quantities were based on the amount of applied carbon of a standard farmyard manure (FYM) application of 12.5 t ha^{-1} a^{-1} (7.5 t ha^{-1} before maize or sorghum and 5 t ha^{-1} before winter rye). The amount of the other organic fertilizers is determined by the amount of organic carbon (Corg) spread by the manure at every application date, so that the amount of Corg is the same for all applied organic fertilizers. The resulting differences in applied nitrogen were balanced by mineral fertilization.

At each plot, five soil samples were taken to a depth of 20 cm two times a year (2011–2020), once after the harvest of green rye in May and then after the harvest of either sorghum or maize in October. The soil was air-dried, sieved (<2 mm) and analysed for soil organic carbon (Dumas) and phosphorus content (double lactate method).

TABLE 1 Soil properties of field trials for the upper 30 cm, the considered period of the trial and fertilizer application

Field trial	Clay (%)	Silt (%)	Sand (%)	Soil pH	Period (years)	CRL (kg ha^{-1} a^{-1})	MIN (kg ha^{-1} a^{-1})	FYM	Location
BL	21	68	11	7	1950–2019	No fertilizer	N: 40–170, P: 0–60	30 t ha^{-1} biennially No P and N	51°23′25.8″N 11°52′49.1″E
BG	1.1	9	89.9	5.54	2011–2022	No fertilizer	N ~ 250, no P	12.5 t ha^{-1} a^{-1} No P and N	52°37′11″N 12°47′16″E
RO	7.65	24.5	67.85	5.64	1999–2014	N: 160, no P	P: 21.8, N: 150–200	30 t ha^{-1} triennially No P and N	54°03′41.6″N 12°05′07.2″E
SP	9	20	71	6	1984–2018	No N, P: 30	P: 30, N: 200–240	30 t ha^{-1} triennially P 30 kg ha^{-1} a^{-1}, No N	49°21′40″N 8°25′14″E

2.1.2 | Bad Lauchstädt (BL)

The Static Fertilization Experiment in Bad Lauchstädt was set up in 1902 on an area of 4 ha, divided into eight fields of which the third was used. The experiment has a systematic design without replications. The analysed plots were fertilized with manure donation of 30 t ha^{-1} every second year. Further, a plot series without any addition of manure was established. Besides the organic fertilization, the plots were further subdivided into plots with mineral fertilization with the addition of NPK and without mineral fertilization. The level of mineral fertilization has been geared to breeding progress from the very beginning. Farmyard manure, P and potassium (K) are applied every 2 years after the harvest of cereals. Cereals receive two mineral N applications: at the beginning of vegetation and at the beginning of tillering. Silage maize is N-fertilized before sowing. N is fertilized as calcium ammonium nitrate, P as triple superphosphate (TSP) and K as 60% potash. The harvested crop, including the by-products, is driven off the field. The crop rotation was sugar beet-spring barley-potato-winter wheat until 2014. In 2015, the sugar beet and potato were replaced by silage maize.

The soil samples were each taken after harvesting with a grooved auger at a depth of 0–20 cm, dried, sieved (2 mm) and analysed (SOC after dry burning-elemental analysis, P double lactate (DL)-extract with photometry/F-AAS). Details can be found in Körschens (2000).

2.1.3 | Rostock (RO)

In autumn 1998, the field trial was established as randomized slit-plot with four replication. Rather than having a fix crop rotation, the field trial was cropped with varying crops, starting in 1999 with spring rape followed by spring barley(2000), spring wheat (2001), spring rape (2002), winter wheat (2003), winter barley (2004) winter rape (2005), maize (2006–2008), sorghum (2009, 2010), sunflower (2011), winter rye (2012) and maize (2013, 2014). Furthermore, intercrops have been cultivated in the years 1999, 2000, 2001 and 2002 with an intercrop mix, 2006 with buckwheat, 2007 with mustard, 2008 with a rye mix and 2009 with green rye.

For this study, the control treatments with no addition of P, the mineral plots with fertilization of TSP, and the plots with cattle manure were chosen. TSP was applied annually at a rate of 21.8 kg P ha^{-1}, while the manure was applied every 3 years at about 30 t ha^{-1} (1998, 2001, 2004, 2007, 2010 and 2013; Zicker et al., 2018).

The soil sampling was carried out twice per year in February/March and September in the upper soil layer (0–30 cm) with four spatial replications (samples from each spatial repetition consisted of 10–15 subsamples). Soil samples were air-dried and sieved (2 mm), and plant-available P was extracted with double lactate solution.

2.1.4 | Speyer

The test site is located in the Upper Rhine valley north of Speyer (Germany) at 99 m above NN. The soil is a cambisol developed from loamy sand with a low field capacity of 10%. The average annual rainfall is 600 mm, and the average annual temperature is 10°C. Because of the low water capacity, the trial is irrigated if necessary.

The field trial was performed within the International Organic Nitrogen Fertilization Experiment (IOSDV) to investigate the interaction of a combination of organic and mineral fertilization. The experiment with a 3 years crop rotation of sugar beet, winter wheat and winter barley was established in 1983. Additionally, since 2004 different soil tillage methods were investigated.

The different fertilization treatments were set up based on a full-factorial design on plots with a size of 6×7.5 m with three replicates for each treatment but with a shifted crop rotation. The chosen plots were fertilized with mineral N application of 0 and 240 kg N ha^{-1} year^{-1} for sugar beet, 0 kg N ha^{-1} year^{-1} for winter wheat and 200 kg N ha^{-1} year^{-1} for winter barley. All plots received P fertilization; therefore, there is no real control plot (CRL*). Farmyard manure was applied at a rate of 30 t ha^{-1} ahead sugar beet. The intercrop received 50 kg ha^{-1} mineral nitrogen fertilizer.

Mineral fertilization with basic nutrients is carried out in all variants in a uniform manner with an average (1984–2018) of 30 kg P ha^{-1} year^{-1}, 118 kg K ha^{-1} year^{-1} and 32 kg Mg ha^{-1} year^{-1}. Details about the field experiment can be found in Körschens (2000).

2.2 | Model description

2.2.1 | C-module

The CNP-model is an enhancement of the CCB model (Franko et al., 2011) where a new P-module is coupled to the C-model of the CCB. The C-module describes the turnover of decomposable carbon in monthly time steps depending on site conditions, crop yields and input rates of FOM. A specific characteristic of the CCB model is the handling of FOM as a list of specific pools from which the C is released to atmosphere or used to build up new SOM. Each FOM entry in that list also comprises a specific C/P ratio. The decomposition is controlled by the FOM-specific parameters k_{fom} describing the FOM breakdown and eta (η) describing the part of C that is transferred to

SOM. First, FOM is moved into the pool of active SOM (A-SOM), which behaves like the microbial biomass that is interacting with the pool of stabilized SOM (S-SOM) and acts as the mineralization driving pool. Additionally, the C-model includes the long-term stabilized pool (LTS-SOM) where SOM is considered as physically protected. All these processes, as well as the FOM turnover, are controlled by site conditions like soil texture, air temperature and rainfall. These conditions are aggregated into a Biologic Active Time (BAT in days [d]) expressing the part time interval that would be required under optimal conditions in the laboratory to produce the same C turnover as under real conditions in the field. Additionally, a matter transfer between A-SOM and LTS pool is considered. A part of the newly built SOM (C_{rep}) is captured inside micropores and thus shielded from decomposition, whereas a part of C-LTS is released from protection and exposed to microbial turnover. Details about the CCB modelling approach and its applications to describe SOM topsoil dynamics were already published (Franko et al., 2011, 2021).

2.2.2 | P-module

The new P-module links the organic P cycle to the C-pools A-SOM, S-SOM and LTS (see Figure 2). When FOM enters the system, a part gets transferred into the SOM pools (Figure 2 (2)), while another part gets mineralized and P is released ($P_{FOM(min)}$) and transferred to the P_{av}-pool (Figure 2 (3)). During C mineralization of the SOM pools, the C assimilated P moves through these pools. The C/P ratio for the SOM pools is assumed to be 186 (Cleveland & Liptzin, 2007). A-SOM ether controls the release of organic P during the mineralization of SOM ($P_{SOM(min)}$; Figure 2 (4)) or the sequestration into a SOM pool with a longer detention time (S-SOM or LTS for detail description see Section 2.2.1).

Additionally, the P-module comprises an available P-pool (P_{av}), which represents the plant-available P species including dissolved P and easily sorbed P. The P_{av}-pool is in an equilibrium with the nonavailable P-pool (P_{na}; Figure 2 (9, 10)). This pool represents the P, which is strongly sorbed to the mineral phase of the soil.

The equilibrium is described by the function:

$$\begin{aligned} PS = {} & 0.6226 + P_{av} * 0.0131 + clay * 0.0214 \\ & - SOC * 0.0621 - \ln(silt) * 0.2085 \end{aligned} \quad (2)$$

Where the function is influenced by the current state of P_{av} and SOC content as well as by the clay and the silt content of the soil. PS represent the relation between P_{av} and P_{na}:

$$PS = \frac{P_{av}}{P_{na}} \quad (3)$$

Where P_{na} can be calculated:

$$P_{na} = P_t - P_{av} - P_{SOM} \quad (4)$$

The observed PS value can be received from measurements with Formulas (3 and 4) with given P_t, P_{av} and SOC values assuming SOM has a C/P ratio of 186. The calculated PS value can be obtained from Formula (2); the relation between those approaches is displayed in Figure 1, which match the identity line.

The plant uptake is withdrawn from the P_{av}-pool (Figure 2 (11)), while the amount is calculated through the production of biomass, distinguishing between main product, by-product, stubble and roots. With the harvest of crops, P (P_{crop}) gets removed (Figure 2 (13)) from the system while stubble and roots enter the P cycle as FOM (Figure 2 (12)). Mineral P fertilizer (P_{fert}) enters with 80% into P_{av} and with 20% into P_{na} (Figure 2 (7, 8)), while a

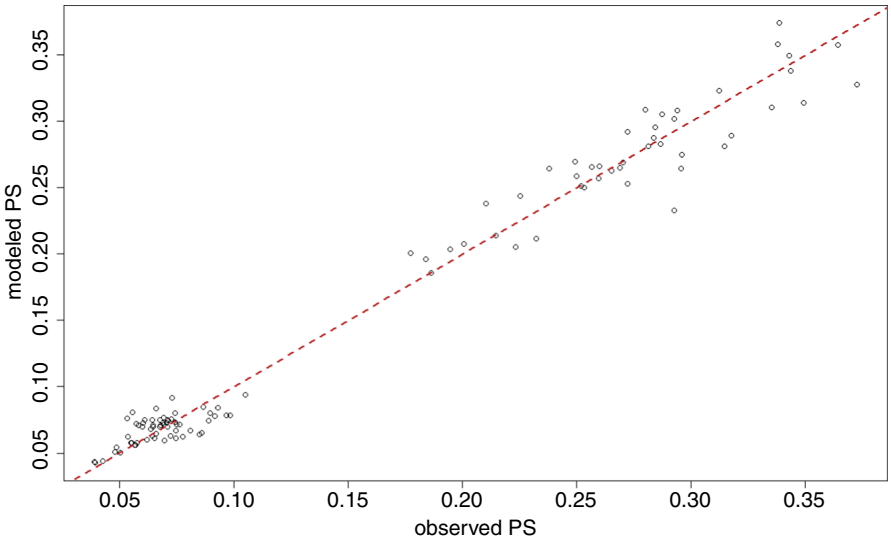

FIGURE 1 Observed PS calculated with Formula (3) and the modelled PS received with Formula (2), red: the identity line (1:1)

constant amount of P enters through weathering (P_w) or deposition directly into the P_{av}-pool (Figure 2 (6)).

On a monthly base (i), the state of the P_{av}-pool is calculated as:

$$P_{av(i+1)} = P_{av(i)} + P_{SOM(min(i))} + P_{FOM(min(i))} + P_{w(i)} + 0.8 * P_{fert(i)} + P_{na(i)} * \kappa - P_{av(i)} * \kappa * z_i - P_{crop(i)} \quad (5)$$

Where κ represents a constant site-specific parameter and z is expressed as:

$$z = \frac{1}{PS} \quad (6)$$

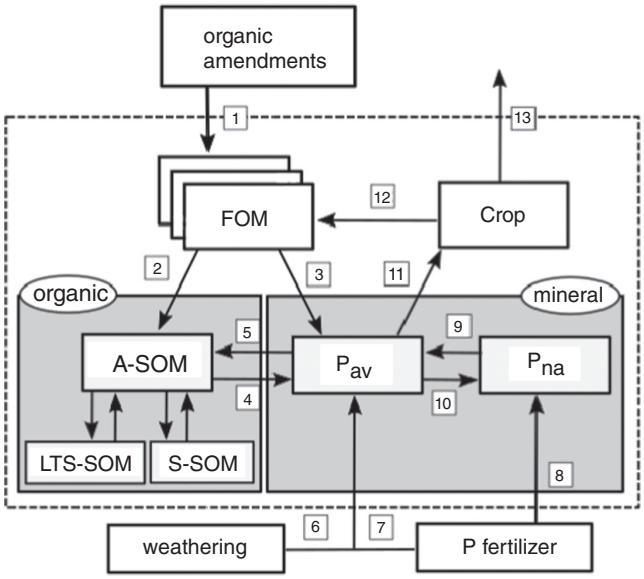

FIGURE 2 Visualization of the P fluxes in the CNP-model; (1) external input of organic amendments like farmyard manure; (2) P transferred from FOM-pools to SOM (A-SOM), (3) P transfer into P_{av} during C mineralization depending on the C/P ratio of FOM; (4) P release during C mineralization of SOM; (5) P uptake of SOM from P_{av} during the build-up of SOM (details in the description of the C-module); (6) P input into P_{av} through weathering; (7) 80% mineral P input into P_{av} through mineral fertilizer; (8) 20% mineral P input into P_{na} through mineral fertilizer; (9) κ, the flux from P_{na} to P_{av} (site specific); (10) the flux from P_{av} to P_{na}, κ*z (z depends on PS); dark grey boxes: total P; (11) crop P uptake into main product, by-product, stubble and roots; (12) FOM-P input through stubble and roots of the crop; (13) P removal with main product and by-product

And the corresponding P_{na} value is calculated with Equation (7):

$$P_{na(i+1)} = P_{na(i)} - P_{na(i)} * \kappa + P_{av(i)} * \kappa * z_i + 0.2 * P_{fert(i)} \quad (7)$$

The total phosphor (P_t) comprises the P_{av}, P_{na} and P_{SOM} pools:

$$P_{t(i+1)} = P_{av(i)} + P_{na(i)} + P_{SOM(i)} \quad (8)$$

2.2.3 | Initialization

The P dynamics depend on the C turnover of the examined soil system. Therefore, the C mineralization has to be initialized first with feasibly good results, to improve the P modelling results. The C-module was initialized by minimizing the mean error, with the integrated function of the CNP-model.

For the initialization, the P-module requires a κ value, which is site specific and was chosen to fit the CRL plots as well as possible, with respect to good results of the other plots. Furthermore, a start value for the P_{av}-pool is required and a P_t value which gets calculated internally if not provided where P_{na} can be calculated from P_{av} and PS:

$$P_{na} = \frac{P_{av}}{PS} \quad (9)$$

P_{SOM} gets calculated according to the distribution of C into the C-pools. The weathering rate was assumed to be 1 kg ha^{-1} a^{-1} except for BL, which was set to 5 kg ha^{-1} a^{-1} (Table 2).

2.2.4 | Parametrization

The C-model requires on the one hand parameters to determine the quality of FOM as well as parameters, which describe the quantity of FOM in terms of the amount of crop residues at a certain yield. The quality of each FOM unit is defined by the dry matter content and the C content, separating FOM into organic fertilizers, by-products which remain on the field, stubble and roots as well as

TABLE 2 κ values for each plot received by optimization and the initial P_{av} and P_t values for the plots

		CRL initial value		MIN initial value		FYM initial value	
LTE	**κ**	**P_{av}**	**P_t**	**P_{av}**	**P_t**	**P_{av}**	**P_t**
BG	0.009	10	48	10	51	10	46
BL	0.002	4	50	4	40	4	63
SP	0.0035	20, 23, 27	43, 42, 44	16, 20, 20	42, 48, 50	23, 20, 26	37, 40, 42
RO	0.011	3.2	60	3.2	58	3.2	60

TABLE 3 Main crop parameters required by the CNP-model, with the dry matter (dm_{mp}), as well as the C and P content (%) of the main product (mp), stubble (st) and roots (rt); C/P ratio of stubble and of the roots; Stix, Fix_s and Rix are the parameters to calculate the amount of stubble in dependence of the main product; Bix and Fix_r describe the amount of roots in dependence of the main product, η_{st} and $k_{fom(st)}$ describe the decomposition of the stubble and η_{rt} and $k_{fom(rt)}$ of the roots

Crop	Main product	Dm_{mp} (%)	P_{mp} (%)	C_{mp} (%)	C_{st} (%)	C_{rt} (%)	C/P_{st} (–)	C/P_{rt} (–)	Stix (–)	Fix_s (dt)	Fix_r (dt)	Bix (–)	Rix (–)	η_{st} (–)	$k_{fom(st)}$ (–)	η_{rt} (–)	$k_{fom(rt)}$ (–)
Maize	Plant	32.9[c]	0.187[b]	42[e]	42	37.8	182.6[f]	317.9[g]	1	0	0	0.0851	0.059	0.313	0.067	0.419	0.124
Potato	Tuber	20.6[a]	0.22[a]	40.4[h]	33	40.7	194.1[h]	145.8[h]	1	0	3.2	0.28	0.14	0.39	0.12	0.54	0.17
Sorghum	Plant	35.1[c]	0.22[bc]	41	41	33.8	136.6[c]	355.4[c]	1	0	0	0.1935	0.107	0.257	0.073	0.456	0.112
Sunflower	Plant	21.6[b]	0.32[ab]	40	43	34.9	165.4[a]	132[g]	1	0	27.9	0.4	0.27	0.39	0.12	0.54	0.17
Spring barley	Grain	86	0.35[b]	40.6	45	35	1006.7[e]	368.4[e]	0.1	0	7.2	0.125	0.85	0.39	0.12	0.54	0.17
Spring rape	Seeds	92.3[a]	0.74[ab]	60	44.9	35	748.3[f]	472.9[g]	0.1	0	13.2	0.19	1.47	2.4	0.71	0.54	0.17
Spring wheat	Grain	86	0.37	44	45.8	35.5	915[f]	593	0.1	0	6	0.088	0.87	0.57	0.2	0.55	0.125
Sugar beet	Tuber	23	0.17	39	31.4	37.9	84.9[a]	222.6[a]	0	5.3	4.7	0	0.55	0.62	0.67	0.54	0.17
Winter barley	Grain	86	0.35[b]	44	45	35	1006.7[e]	368.4[e]	0.1	0	9.3	0.13	0.84	0.39	0.12	0.54	0.17
Green rye	Plant	22.9[c]	0.44[b]	43[d]	42	35.6	330.7	273.8	1	0	0	0.257	0.097	0.257	0.07	0.57	0.139
Winter rape	Seeds	92.3[a]	0.60[b]	60	44.9	35	748.3[f]	472.9[g]	0.1	0	4.6	0.179	1.58	2.4	0.71	0.17	0.54
Winter wheat	Grain	86	0.31[b]	40.6[e]	45.8	35.5	915[f]	593.3[e]	0.1	0	11.6	0.16	0.93	0.57	0.2	0.55	0.125
Oil radish	Catch crop	15	0.168	43	43	35	256[j]	208[j]	0	4.68	7.0	0	0	0.39	0.12	0.54	0.17
Mustard	Catch crop	15	0.35	43	43	35	198[i]	194[i]	0	4.1	7.6	0	0	0.39	0.12	0.54	0.17
Buckwheat	Catch crop	15.9[a]	0.24[a]	43	43	35	179[a]	145	0	4.4	6.6	0	0	0.39	0.12	0.54	0.17

Source: [a]Feedipedia – Animal Feed Resources Information System; [b]Measurements LTE RO; [c]Measurements LTE BG; [d]Mewes (2017); [e]Measurements LTE BL; [f]Max et al. (2022); [g]Calculated with Formula (8); [h]Chea et al. (2021); [i]Hallama et al. (2022); [j]Mann et al. (2021).

the incorporation of catch crops. Furthermore, the quality is described by the FOM-specific mineralization parameters of the CNP-model. With k_{fom} which is the turnover coefficient of FOM and η the synthesis coefficient which describes the relation between CO_2 release to the composition of A-SOM. Furthermore, the C/P ratio of each FOM unit is required. The quantification of Crop input is described by linear functions between the main product and the corresponding amount of by-product, stubble and roots (Franko et al., 2021; Gasser et al., 2022). This is of importance for the SOM cycle and for the organic P cycling in the model. The input of each FOM unit needs to be specified and can have different parameters for the mineralization as well as for the chemical composition, resulting in different qualities for each FOM input. Furthermore, for each FOM input, the C/P ratio of the stubble and roots needs to be defined. An overview of the used parameters is given in Table 3.

The total P content of the stubble and the roots of four crops were harvested and analysed internally in a laboratory. This was done for winter wheat and spring barley in BL and for sorghum and green rye in BR. The linear regression is shown in Figure 3 and Equation (10) (residual error = 0.47 [g kg^{-1}]). For plants with lacking information about the P content in roots, the regression was used as approximation to calculate the amount of P in the roots in accordance with the amount of P in the stubble.

$$P_{root\ (g\ kg^{-1})} = 0.17186 + P_{stubble\ (g\ kg^{-1})} * 0.9472 \quad (10)$$

The k_{fom} and η values were determined by the modelling of incubated organic material, where the CO_2 release was measured over time; for details, see Gasser et al. (2021, 2022). If no incubation data for a specific crop residue or roots were available, the average of either all available stubble or roots was used. The average parameters for stubble are $k_{fom(st)} = 0.12$ and $\eta_{st} = 0.39$ ($N = 13$), while for roots, the average was used of incubated fine roots ($N = 12$) and coarse roots ($N = 7$) with $k_{fom(rt)} = 0.17$ and $\eta_{rt} = 0.54$.

The farmyard manure was parametrized according to the data of the average FYM applied on the corresponding LTEs (Table 4).

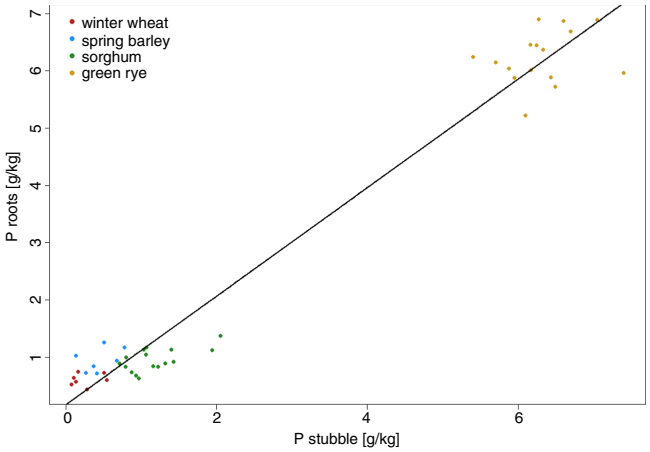

FIGURE 3 Relation between P in stubble and roots of four crops (red: winter wheat, blue: spring barley, green: sorghum, orange: green rye)

TABLE 4 Model parameter for FYM, the dry matter content (dm), carbon content, the C/P ratio and the mineralization parameter k_{fom} and η for all LTEs

LTE	dm (%)	C (%)	C/P ratio	k_{fom}	η
BG	23.7	32.1	45.1	0.095	0.67
BL	27	37.9	56.3	0.114	0.64
RO	28	39	53.5	0.123	0.67
SP	31	39	79.6	0.123	0.67

2.3 | Statistical analysis

The goodness of fit was evaluated by the root mean squared error (RMSE, Equation 11), and furthermore, the relative RMSE (rRMSE, Equation 12) was calculated to characterize the differences between observed values (O) and predicted values (V), with $\overline{O}$ as mean of the observations:

$$RMSE = \sqrt{\frac{\sum_{i=1}^{n}(O_i - V_i)^2}{n}} \quad (11)$$

$$rRMSE = \frac{100}{\overline{O}}\sqrt{\frac{\sum_{i=1}^{n}(O_i - V)^2}{n}} \quad (12)$$

3 | RESULTS

3.1 | Available P dynamics

The model results are displayed in the following section. In BG, the overall trend for P_{av} shows a decrease over the observed period. The CRL plot shows higher P_{av} values than the MIN plot, which can be attributed to the higher removal of P_{av} because of higher crop yields (Figure 4).

In BL, the difference between P_{av} at the CRL and FYM plot is relatively (4–15 mg 100 g^{-1}) big compared with the other LTE, which can be due to the long experimental set-up. Especially in the early years of the LTE, the model overestimates the P_{av} dynamics. On the MIN plot, the

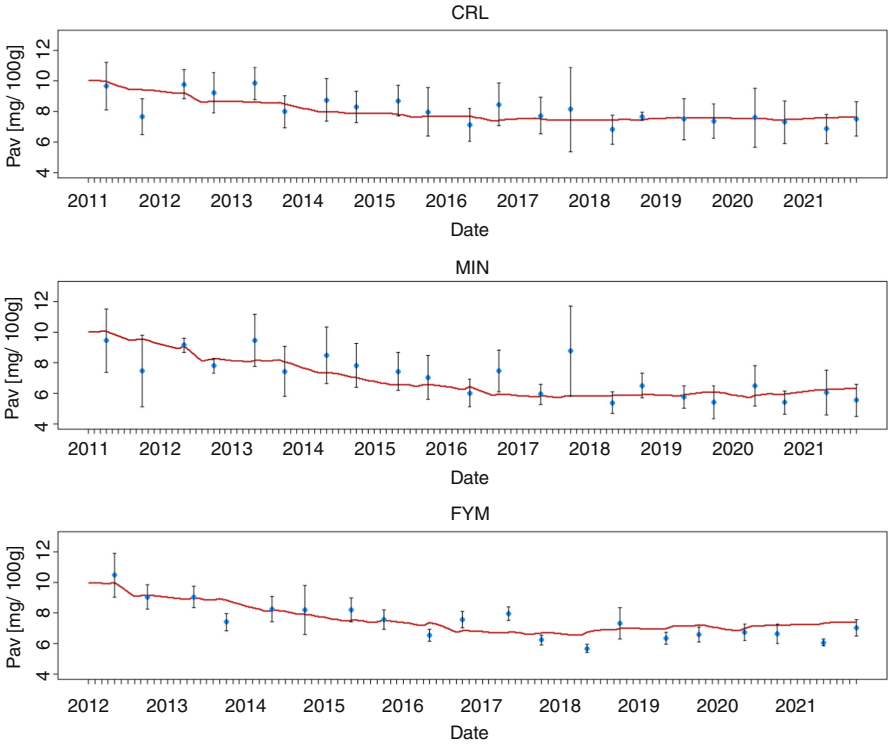

FIGURE 4 P_{av} dynamics for BG, blue mean of transformed DL-P to CAL-P measurements with standard deviation ($N = 4$), red modelled P_{av} values.

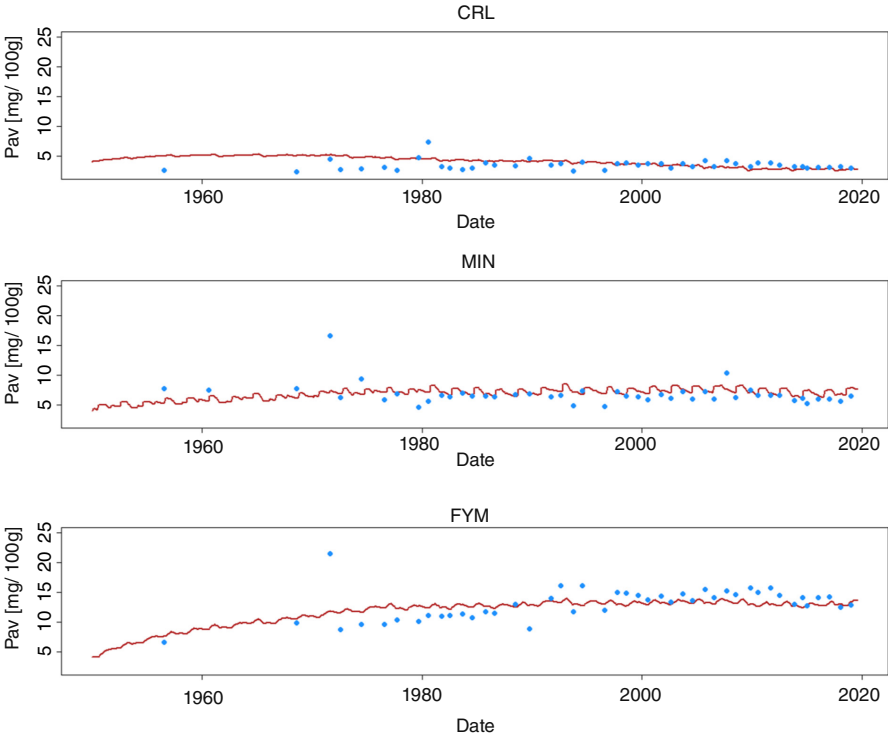

FIGURE 5 P_{av} dynamics for BL, blue transformed DL-P to CAL-P values ($N = 1$), red modelled P_{av}

P-CAL dynamics stay constant despite continuous P fertilization (Figure 5).

The plots in RO show the lowest P_{av} values, while P_{av} seems to decrease at the CRL plot it stays at the same level for MIN and FYM and no big differentiation between the plots is visible (Figure 6).

The CRL* plot in SP shows higher P_{av} and P-CAL values compared with the MIN plot; this could be because of the higher yield and the corresponding P uptake achieved with N-fertilization. The FYM plot shows the highest P_{av} and P-CAL values since it receives mineral P fertilization and organic P fertilization (Figure 7).

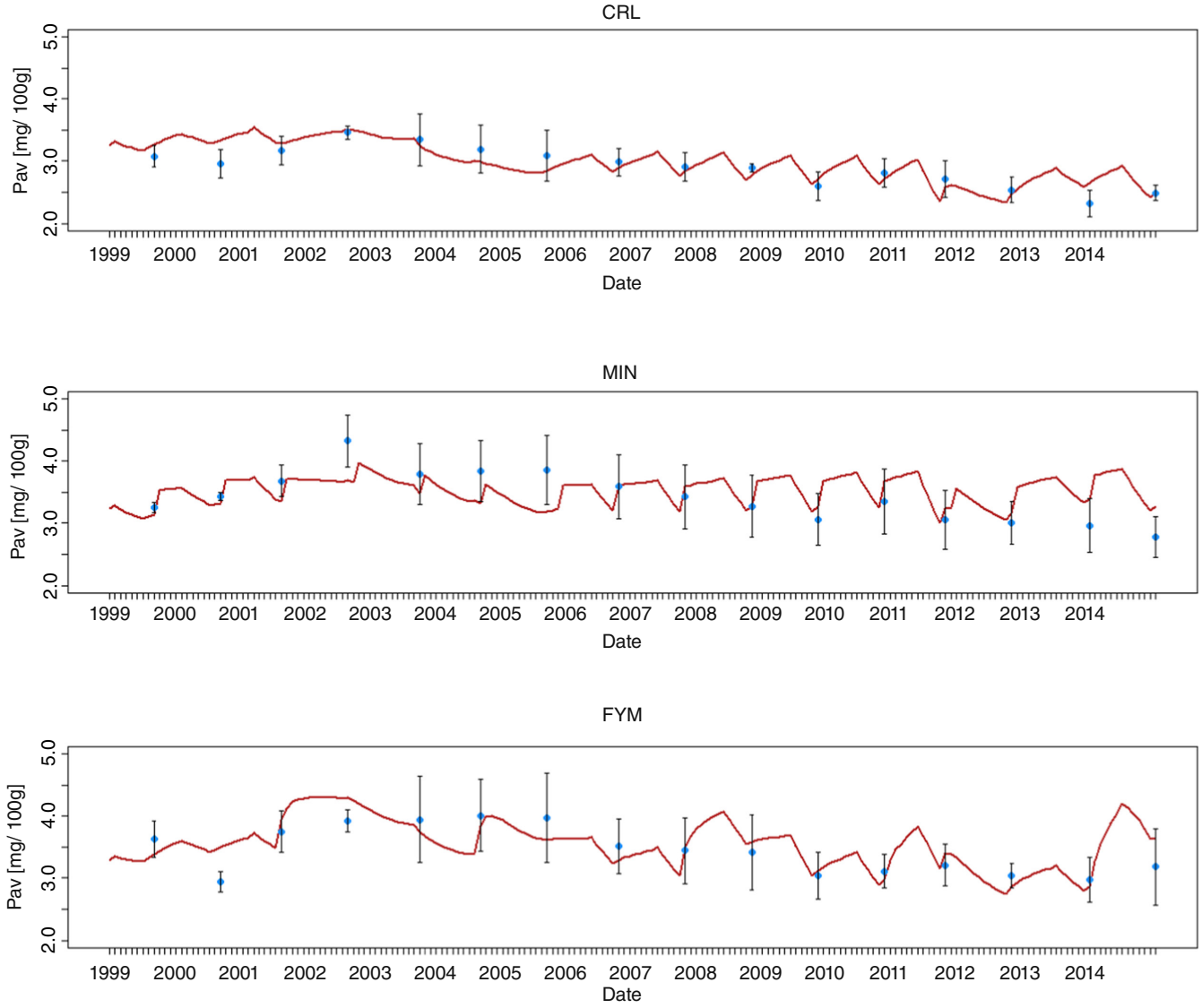

FIGURE 6 P_{av} dynamics of RO, blue mean transformed DL-P to CAL-P measurements with standard deviation ($N = 3$), red modelled P_{av}

The model performance for all analysed plots for P_{av} and Corg is displayed in Table 5. If replicates were available, the RMSE to the mean was calculated. Since SP has a shifted crop rotation in the treatments, each plot was simulated separately and the mean of the RMSE and rRMSE was used over all plots with the same fertilization. The RMSE for P_{av} increases with soil high in P_{av} values.

3.2 | Total P dynamics

Besides the plant-available P, the P-module calculates the P_t dynamics. Due to limited timelines of P_t measurements, only two plots were evaluated, namely the CTR and MIN Plot of RO (Figure 8). The corresponding RMSE for CRL is 1.0 and the rRMSE = 1.8 and, respectively, RMSE = 2.5 and rRMSE = 4.2, for the MIN plot.

4 | DISCUSSION

To make statements about the performance of the P-module, the model results of the carbon module have to be in an adequate range. For all analysed plots of all LTEs, the rRMSE for Corg is below 10%, which lies in a good range compared with other studies (Begum et al., 2017; Guillaume et al., 2021).

The P-model shows an rRMSE of around 10% for most plots. To mention is that in BL the P-model is worse in terms of the rRMSE, compared with all the other LTEs. The reasons for that are amongst others the high variability in the measurements between 2 years. Furthermore, BL shows the highest silt and SOC (1.5%–2%) content of all LTEs, which might result in soil P processes which are not fully covered by the CNP-model. The measured CAL-P values of the CRL plot in BL stay constant over the observed period with no entry of P fertilizer. Either the total

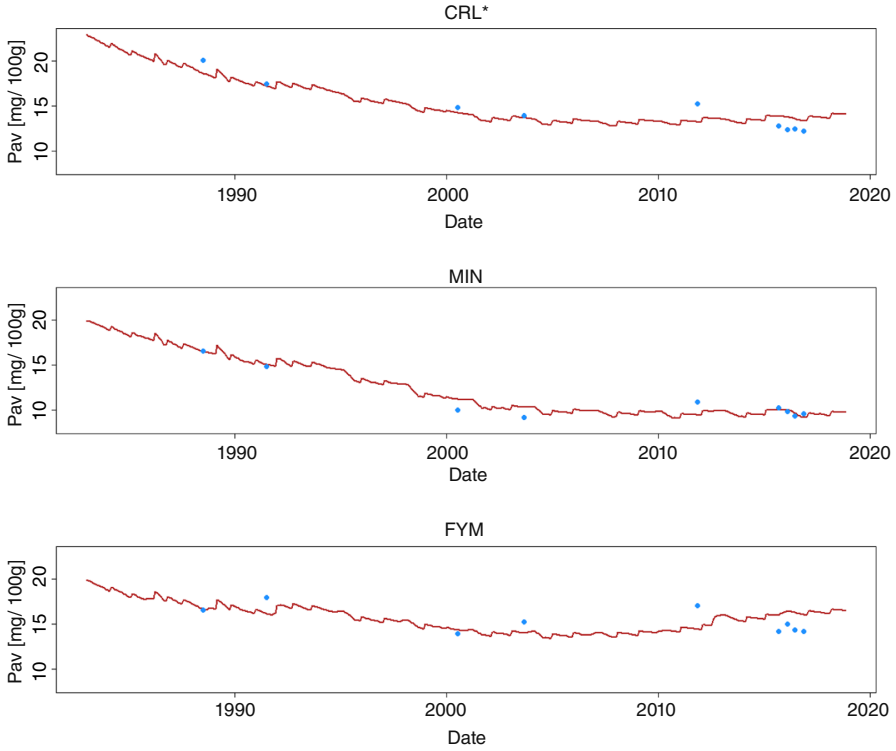

FIGURE 7 P_{av} dynamics of SP, blue CAL-P measurements ($N = 1$), red modelled P_{av}

TABLE 5 Aggregated statistics, RMSE of P_{av} values (mg 100 g^{-1}), the standard deviation (SD) of P-CAL measurements (mg 100 g^{-1}) if replicates are available and the relative RMSE (%); RMSE (mg/100) and relative RMSE (%) for Corg

Plot	LTE	RMSE P_{av}	rRMSE P_{av}	SD P-CAL	RMSE Corg	rRMSE Corg
CRL	BG	0.68	8.42	1.26	0.04	5.83
MIN	BG	1.04	14.65	1.29	0.04	6.8
FYM	BG	0.7	9.43	0.66	0.06	8.75
CRL	RO	0.18	6.08	0.23	0.04	2.72
MIN	RO	0.35	10.34	0.40	0.03	2.11
FYM	RO	0.26	7.7	0.42	0.03	1.93
CRL	BL	1.11	31.93	-	0.13	9.02
MIN	BL	1.87	27.73	-	0.12	6.57
FYM	BL	2.27	17.46	-	0.13	6.10
CRL*	SP	1.6	8.87	-	0.05	8.46
MIN	SP	1.15	9.38	-	0.05	6.15
FYM	SP	2.43	12.86	-	0.07	9.51

P-pool is declining over time strongly, or there might be a bigger P input of unknown sources or plant uptake is withdrawn from deeper soil layers (Pothuluri et al., 1986; Siebers et al., 2021). In the LTE of BG and RO, where replicates were available, the RMSE is lower than the standard deviation of the measured CAL-P values.

For most plots, a time series for P_t was not available, solely a single measurement, where the modelled P_t values are in a close range. For RO, the P_t timeline is modelled with good results, representing the trend with low RMSE and rRMSE. This enables the evaluation of the total P stock of soils and to determine whether the P stocks are increasing or declining and provides information about the potentially available P resources in the soil.

Several studies have shown that P cycling is influenced by erosion and leaching into deeper soil layers (Andersson et al., 2015; Ulén et al., 2007). Subject of the CNP-model is the cultivation layer, the upper 25 cm of the soil. The model does not consider transport mechanisms into deeper soil layers and comprises no water model or an erosion estimate like the Universal Soil Loss Equation, which would be essential for erosion and leaching processes (Reid et al., 2018). In favour of simplicity and a low-threshold model approach, leaching and erosion was not considered yet, because more data input and parametrizations would be required and eventually lead to equifinality.

Yet, another influential factor on P sorption and desorption processes is the pH value of the soil. With an

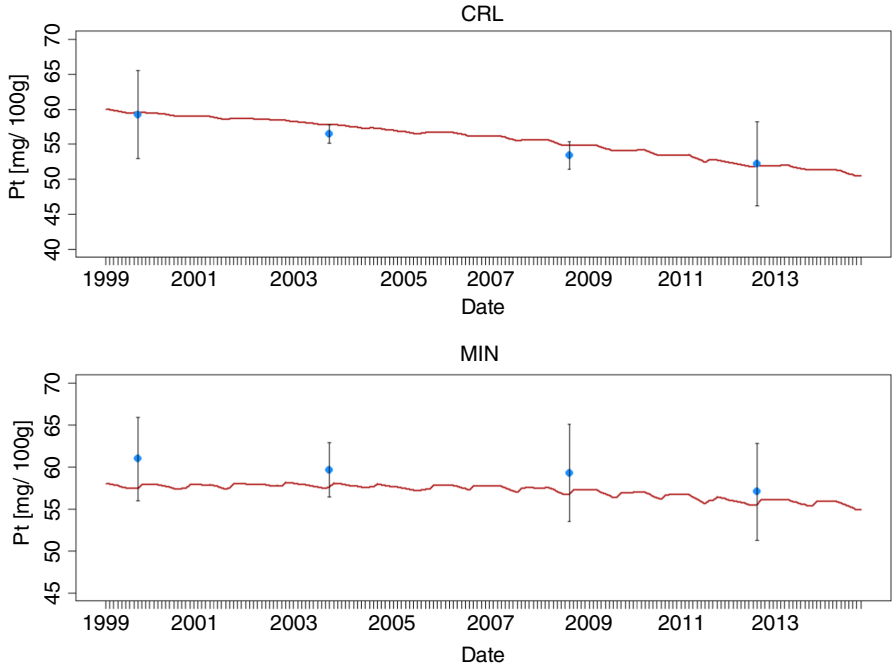

FIGURE 8 Total P dynamic, blue: aqua regia digested P of the CRL and MIN plot of RO with standard deviation ($N = 3$), red modelled P_t

increasing pH value, P gets sorbed to Ca^+ Ions, while with deceasing pH value, the Ca-bound P gets released again and at pH values of around 5 sorption processes to Fe^- and AL^+ complexes gain more importance (Haynes, 1984; McLaughlin et al., 2011; Nobile et al., 2020). Agricultural soils are highly managed soils where the pH value gets regulated to maintain optimal productivity. Therefore, changes in pH value do not play a decisive role for the model scope and have not been considered in the first version of the P-module.

Cleveland and Liptzin (2007) reported a mean global C/P ratio of microbial biomass of 60. Other studies assume that the C/P ratio in microbial biomass is not homeostatic, because of population size-dependent scaling, habitat and ecosystem differences, or shifts in microbial community composition (McConnell et al., 2020). For the current model version, the C/P ratio of all SOM pools is assumed to be 186, but since the CNP-model comprises the A-SOM pool, which behaves like microbial biomass the C/P ratios could be further distinguished.

The PS formula is derived from the four experimental sites, which comprise four soils. Under certain conditions, especially with high silt and SOC contents and low P_{av} and clay contents, the PS formula can get negative and lead to an undefined PS value. Further experiments are required to validate and improve the PS formula. Moreover, with diverse soil properties, further influential parameters might be required to cover all soils with their attributes. Nevertheless, the two-pool model presented here can be used to model the P dynamics on different sites, with varying soil properties, diverse crop rotations and management practices such as intercropping, organic or inorganic fertilization. As organic bound P can have a decisive influence on the P turnover processes, the C dynamics have to be considered and the modelling of the C dynamics has to be precise to grand good results.

The CNP-model can be initialized with the measurable P values P-CAL and P_t. Furthermore, the model output is equivalent to those measurable P species and can be directly compared. While other models like APSIM (Agricultural Production Systems Simulator) and EPIC (erosion-productivity impact calculator) include a sophisticated organic P cycling, the plant-available P-pool does not correspond to a measurable P species (Das et al., 2019) or does not even show a correlation to measurable P species (Raymond et al., 2021). This lowers the predictive use as well as the practical application of such models to consult farmers or other stakeholders.

Compared with APLE, DDPS and LePA, the CNP-model differentiates in detail between the FOM inputs (organic amendments/fertilizer, by-products, stubbles, roots and catch crops). Every input can be characterized in terms of quality like P content or mineralization characteristics. This is also considered in the organic P cycling of the CNP-model, where P release during mineralization of SOM as well as fixation during SOM build-up is considered. This grants a high model flexibility and an overall wide application range. As stated by Damon et al. (2014), crop residues can have a significant influence on P availability by high amounts and high concentrations. Furthermore, the application of a higher variety of organic fertilizers, like digestates or composts is expected, which have a different mineralization behaviour and P availability.

The CNP-model can model the P dynamics of different soil with varying management. This demonstrates the potential of the model to simulate different scenarios. Those scenarios may include different management strategies, like intercropping, the use of digestates or sewage sludges

as organic fertilizers or even a reduction of P fertilizers and the long-term effects on soil P.

5 | CONCLUSION

The CNP-model is a model with few data inputs and the possibility to model the C, N and now the available and total P dynamics of arable soils. The data input is kept low enough that the required data can be provided by farmers from their management practices and yields. The two-pool model presented can be used to model the P dynamics on different sites, with varying soil properties, diverse crop rotations and management practices such as intercropping, organic or inorganic fertilization. As organic bound P can have a decisive influence on the P turnover processes, the C dynamics must be considered and the modelling of the C dynamics has to be precise to grand good results. The P-model initialization and output is equivalent to measurable P species, which makes the output easy to interpret and comparable to measurements. Moreover, a comprehensive list of model parameters comprising common crops is presented. Nevertheless, further field trials need to be modelled and used to validate the P-model concept and to improve model processes.

ACKNOWLEDGEMENTS

This project was funded by the Agency of Renewable Resources (FNR) on behalf of the German Ministry of Food and Agriculture, thank you. The investigation of soil characteristics were partly supported by the project InnoSoilPhos (Federal Ministry of Education and Research No. 031B0509A). Open Access funding enabled and organized by Projekt DEAL.

DATA AVAILABILITY STATEMENT

The data that support the findings of this study are available from the corresponding author upon reasonable request.

ORCID

S. Anton A. Gasser https://orcid.org/0000-0002-4188-1217

REFERENCES

Alewell, C., Ringeval, B., Ballabio, C., Robinson, D. A., Panagos, P., & Borrelli, P. (2020). Global phosphorus shortage will be aggravated by soil erosion. *Nature Communications*, *11*(1), 4546. https://doi.org/10.1038/s41467-020-18326-7

Andersson, H., Bergström, L., Ulén, B., Djodjic, F., & Kirchmann, H. (2015). The role of subsoil as a source or sink for phosphorus leaching. *Journal of Environmental Quality*, *44*(2), 535–544. https://doi.org/10.2134/jeq2014.04.0186

Begum, K., Kuhnert, M., Yeluripati, J., Glendining, M., & Smith, P. (2017). Simulating soil carbon sequestration from long term fertilizer and manure additions under continuous wheat using the DailyDayCent model. *Nutrient Cycling in Agroecosystems*, *109*(3), 291–302. https://doi.org/10.1007/s10705-017-9888-0

Chea, L., Meijide, A., Meinen, C., Pawelzik, E., & Naumann, M. (2021). Cultivar-dependent responses in plant growth, leaf physiology, phosphorus use efficiency, and tuber quality of potatoes under limited phosphorus availability conditions. *Frontiers in Plant Science*, *12*. https://doi.org/10.3389/fpls.2021.723862.

Cleveland, C. C., & Liptzin, D. (2007). C:N:P stoichiometry in soil: Is there a "Redfield ratio" for the microbial biomass? *Biogeochemistry*, *85*(3), 235–252. https://doi.org/10.1007/s10533-007-9132-0

Damon, P. M., Bowden, B., Rose, T., & Rengel, Z. (2014). Crop residue contributions to phosphorus pools in agricultural soils: A review. *Soil Biology and Biochemistry*, *74*, 127–137. https://doi.org/10.1016/j.soilbio.2014.03.003

Das, B., Huth, N., Probert, M., Condron, L., & Schmidt, S. (2019). Soil phosphorus modeling for modern agriculture requires balance of science and practicality: A perspective. *Journal of Environmental Quality*, *48*(5), 1281–1294. https://doi.org/10.2134/jeq2019.05.0201

Dzombak, R. M., & Sheldon, N. D. (2020). Weathering intensity and presence of vegetation are key controls on soil phosphorus concentrations: Implications for past and future terrestrial ecosystems. *Soil Systems*, *4*(4), 73. https://doi.org/10.3390/soilsystems4040073

Feedipedia – Animal Feed Resources Information System. INRA, CIRAD, AFZ and FAO. Retrieved July 1, 2022, from https://www.feedipedia.org/

Franko, U., Diel, J., & Ruehlmann, J. (2021). Applying CCB to predict management change affected long-term SOM turnover of the extended static fertilization experiment in Bad Lauchstädt. *European Journal of Soil Science*, *73*, e13148. https://doi.org/10.1111/ejss.13148

Franko, U., Kolbe, H., Thiel, E., & Ließ, E. (2011). Multi-site validation of a soil organic matter model for arable fields based on generally available input data. *Geoderma*, *166*(1), 119–134. https://doi.org/10.1016/j.geoderma.2011.07.019

Gasser, S. A. A., Diel, J., Nielsen, K., Mewes, P., Engels, C., & Franko, U. (2021). A model ensemble approach to determine the humus building efficiency of organic amendments in incubation experiments. *Soil Use and Management*, *38*, 179–190. https://doi.org/10.1111/sum.12699

Gasser, S. A. A., Nielsen, K., & Franko, U. (2022). Transfer of carbon incubation parameters to model the SOC and SO dynamics of a field trial with energy crops applying digestates as organic fertilizers. *Soil Use and Management*, 1-15. https://doi.org/10.1111/sum.12810

Guillaume, T., Bragazza, L., Levasseur, C., Libohova, Z., & Sinaj, S. (2021). Long-term soil organic carbon dynamics in temperate cropland-grassland systems. *Agriculture, Ecosystems & Environment*, *305*, 107184. https://doi.org/10.1016/j.agee.2020.107184

Hadjipanayiotou, M., Economides, S., & Koumas, A. (1985). *Chemical composition, digestibility and energy content of leguminous grains and straws grown in a Mediterranean region*. Paper presented at the Annales de Zootechnie.

Hallama, M., Pekrun, C., Mayer-Gruner, P., Uksa, M., Abdullaeva, Y., Pilz, S., Schloter, M., Lambers, H., & Kandeler, E. (2022). The role of microbes in the increase of organic phosphorus availability in the rhizosheath of cover crops. *Plant and Soil*, *476*, 353–373. https://doi.org/10.1007/s11104-022-05340-5

Haynes, R. J. (1984). Lime and phosphate in the soil-plant system. *Advances in Agronomy*, *37*, 249–315. https://doi.org/10.1016/s0065-2113(08)60456-3

Körschens, M. (2000). *IOSDV Internationale organische Stickstoffdauerdüngungsversuche*. Bericht der Internationalen Arbeitsgemeinschaft Bodenfruchtbarkeit in der Internationalen Bodenkundlichen Union (IUSS), UFZ-Bericht, 15, 2000.

Mann, T., Heckelmann, A., Uckele, H., Jilg, T., Elsäßer, M., Messner, J., Zacharias, B., Roth, U., Vollmer, K.-H., Rather, K., Riedel, M., & Rupp, D. (2021). *Stammdatensammlung*. Retrieved from www.ltz-augustenberg.de

Max, P., Martin, A., & Franz, W. (2022). *Verbundvorhaben: Bewertung der Humus- und Nährstoffwirkung von organischen Reststoffen; Teilvorhaben 2: Chemische Charakterisierung der Reststoffe und Ermittlung von deren N- und P-Dynamik in Inkubationsversuchen*. Retrieved from https://www.fnr.de/index.php?id=11150&fkz=22410918

McConnell, C. A., Kaye, J. P., & Kemanian, A. R. (2020). Reviews and syntheses: Ironing out wrinkles in the soil phosphorus cycling paradigm. *Biogeosciences*, *17*(21), 5309–5333. https://doi.org/10.5194/bg-17-5309-2020

McLaughlin, M. J., McBeath, T. M., Smernik, R., Stacey, S. P., Ajiboye, B., & Guppy, C. (2011). The chemical nature of P accumulation in agricultural soils—Implications for fertiliser management and design: An Australian perspective. *Plant and Soil*, *349*(1–2), 69–87. https://doi.org/10.1007/s11104-011-0907-7

Mewes, P. (2017). *Persistence of exogenous organic matter in soil as a cultivation property*. [PhD Dissertation, Humboldt-University of Berlin].

Nobile, C. M., Bravin, M. N., Becquer, T., & Paillat, J. M. (2020). Phosphorus sorption and availability in an andosol after a decade of organic or mineral fertilizer applications: Importance of pH and organic carbon modifications in soil as compared to phosphorus accumulation. *Chemosphere*, *239*, 124709. https://doi.org/10.1016/j.chemosphere.2019.124709

Pothuluri, J., Kissel, D., Whitney, D., & Thien, S. (1986). Phosphorus uptake from soil layers having different soil test phosphorus levels 1. *Agronomy Journal*, *78*(6), 991–994. https://doi.org/10.2134/agronj1986.00021962007800060012x

Raymond, N., Kopittke, P. M., Wang, E., Lester, D., & Bell, M. J. (2021). Does the APSIM model capture soil phosphorus dynamics? A case study with Vertisols. *Field Crops Research*, *273*, 108302.

Reid, K., Schneider, K., & McConkey, B. (2018). Components of phosphorus loss from agricultural landscapes, and how to incorporate them into risk assessment tools. *Frontiers in Earth Science*, *6*, 135. https://doi.org/10.3389/feart.2018.00135

Sattari, S. Z., Bouwman, A. F., Giller, K. E., & van Ittersum, M. K. (2012). Residual soil phosphorus as the missing piece in the global phosphorus crisis puzzle. *Proceedings of the National Academy of Sciences of the United States of America*, *109*(16), 6348–6353. https://doi.org/10.1073/pnas.1113675109

Siebers, N., Wang, L., Funk, T., von Tucher, S., Merbach, I., Schweitzer, K., & Kruse, J. (2021). Subsoils—A sink for excess fertilizer P but a minor contribution to P plant nutrition: Evidence from long-term fertilization trials. *Environmental Sciences Europe*, *33*(1), 1–19. https://doi.org/10.1186/s12302-021-00496-w

Sulieman, S., & Mühling, K. H. (2021). Utilization of soil organic phosphorus as a strategic approach for sustainable agriculture. *Journal of Plant Nutrition and Soil Science*, *184*(3), 311–319. https://doi.org/10.1002/jpln.202100057

Ulén, B., Bechmann, M., Fölster, J., Jarvie, H., & Tunney, H. (2007). Agriculture as a phosphorus source for eutrophication in the north-west European countries, Norway, Sweden, United Kingdom and Ireland: A review. *Soil Use and Management*, *23*, 5–15. https://doi.org/10.1111/j.1475-2743.2007.00115.x

Vadas, P. A., Joern, B. C., & Moore, P. A. (2012). Simulating soil phosphorus dynamics for a phosphorus loss quantification tool. *Journal of Environmental Quality*, *41*(6), 1750–1757. https://doi.org/10.2134/jeq2012.0003

van Laak, M., Klingenberg, U., Peiter, E., Reitz, T., Zimmer, D., & Buczko, U. (2018). The equivalence of the calcium-acetate-lactate and double-lactate extraction methods to assess soil phosphorus fertility. *Journal of Plant Nutrition and Soil Science*, *181*(5), 795–801. https://doi.org/10.1002/jpln.201700366

Vet, R., Artz, R. S., Carou, S., Shaw, M., Ro, C.-U., Aas, W., Baker, A., Bowersox, V. C., Dentener, F., Galy-Lacaux, C., Hou, A., Pienaar, J. J., Gillett, R., Forti, M. C., Gromov, S., Hara, H., Khodzher, T., Mahowald, N. M., Nickovic, S., … Reid, N. W. (2014). A global assessment of precipitation chemistry and deposition of sulfur, nitrogen, sea salt, base cations, organic acids, acidity and pH, and phosphorus. *Atmospheric Environment*, *93*, 3–100. https://doi.org/10.1016/j.atmosenv.2013.10.060

Wang, Y., Bauke, S. L., von Sperber, C., Tamburini, F., Guigue, J., Winkler, P., Kaiser, K., Honermeier, B., & Amelung, W. (2021). Soil phosphorus cycling is modified by carbon and nitrogen fertilization in a long-term field experiment. *Journal of Plant Nutrition and Soil Science*, *184*(2), 282–293. https://doi.org/10.1002/jpln.202000261

Wuenscher, R., Unterfrauner, H., Peticzka, R., & Zehetner, F. (2016). A comparison of 14 soil phosphorus extraction methods applied to 50 agricultural soils from Central Europe. *Plant, Soil and Environment*, *61*(2), 86–96. https://doi.org/10.17221/932/2014-pse

Yan, X., Li, G., Zhang, W., Muneer, M. A., Yu, W., Ma, C., & Wu, L. (2022). Spatio-temporal variation of soil phosphorus and its implications for future pomelo orcharding system management: A model prediction from Southeast China from 1985–2100. *Frontiers in Environmental Science*, *10*, 816. https://doi.org/10.3389/fenvs.2022.858816

Yu, W., Li, G., Hartmann, T. E., Xu, M., Yang, X., Li, H., Zhang, J., & Shen, J. (2021). Development of a novel model of soil legacy P assessment for calcareous and acidic soils. *Frontiers in Environmental Science*, *8*, 833. https://doi.org/10.3389/fenvs.2020.621833

Zhang, J., Beusen, A. H., Van Apeldoorn, D. F., Mogollón, J. M., Yu, C., & Bouwman, A. F. (2017). Spatiotemporal dynamics of soil phosphorus and crop uptake in global cropland during the 20th century. *Biogeosciences*, *14*(8), 2055–2068. https://doi.org/10.5194/bg-14-2055-2017

Zicker, T., von Tucher, S., Kavka, M., & Eichler-Löbermann, B. (2018). Soil test phosphorus as affected by phosphorus budgets in two long-term field experiments in Germany. *Field Crops Research*, *218*, 158–170. https://doi.org/10.1016/j.fcr.2018.01.008

How to cite this article: Gasser, S. A. A., Nielsen, K., Eichler-Löbermann, B., Armbruster, M., Merbach, I., & Franko, U. (2023). Simulating the soil phosphorus dynamics of four long-term field experiments with a novel phosphorus model. *Soil Use and Management*, *39*, 867–880. https://doi.org/10.1111/sum.12881